Modelling and characterisation of a ultrasound-actuated needle for improved visibility in ultrasound-guided regional anaesthesia and tissue biopsy

Kuang, Y.; Hilgers, A.; Sadiq, M.; Cochran, S.; Corner, G.; Huang, Z.

Published in:
Ultrasonics

DOI:
10.1016/j.ultras.2016.02.018

Publication date:
2016

Ultrasonics 69 (2016) 38–46

Contents lists available at ScienceDirect

Ultrasonics

journal homepage: www.elsevier.com/locate/ultras

Modelling and characterisation of a ultrasound-actuated needle for improved visibility in ultrasound-guided regional anaesthesia and tissue biopsy

Y. Kuang [a], A. Hilgers [a], M. Sadiq [a], S. Cochran [b], G. Corner [c], Z. Huang [a,*]

[a] School of Science and Engineering, University of Dundee, Dundee DD1 4HN, Scotland, UK
[b] Institute for Medical Science and Technology (IMSaT), University of Dundee, Dundee DD2 1FD, UK
[c] Department of Medical Physics, Ninewells Hospital, University of Dundee, DD1 9SY, UK

ARTICLE INFO

Article history:
Received 7 January 2016
Received in revised form 25 February 2016
Accepted 26 February 2016
Available online 3 March 2016

Keywords:
Needle visibility
Colour Doppler imaging
Regional anaesthesia
Tissue biopsy
Piezoelectric transducer

ABSTRACT

Clear needle visualisation is recognised as an unmet need for ultrasound guided percutaneous needle procedures including regional anaesthesia and tissue biopsy. With inadequate needle visibility, these procedures may result in serious complications or a failed operation. This paper reports analysis of the modal behaviour of a previously proposed ultrasound-actuated needle configuration, which may overcome this problem by improving needle visibility in colour Doppler imaging. It uses a piezoelectric transducer to actuate longitudinal resonant modes in needles (outer diameter 0.8–1.2 mm, length > 65 mm). The factors that affect the needle's vibration mode are identified, including the needle length, the transducer's resonance frequency and the gripping position. Their effects are investigated using finite element modelling, with the conclusions validated experimentally. The actuated needle was inserted into porcine tissue up to 30 mm depth and its visibility was observed under colour Doppler imaging. The piezoelectric transducer is able to generate longitudinal vibration with peak-to-peak amplitude up to 4 μm at the needle tip with an actuating voltage of 20 V_{pp}. Actuated in longitudinal vibration modes (distal mode at 27.6 kHz and transducer mode at 42.2 kHz) with a drive amplitude of 12–14 V_{pp}, a 120 mm needle is delineated as a coloured line in colour Doppler images, with both needle tip and shaft visualised. The improved needle visibility is maintained while the needle is advanced into the tissue, thus allowing tracking of the needle position in real time. Moreover, the needle tip is highlighted by strong coloured artefacts around the actuated needle generated by its flexural vibration. A limitation of the technique is that the transducer mode requires needles of specific lengths so that the needle's resonance frequency matches the transducer. This may restrict the choice of needle lengths in clinical applications.

1. Introduction

Percutaneous needle procedures are common clinical operations for diagnosis and local therapy. Their most widespread applications are regional anaesthesia [1] and tissue biopsy [2], with approximately 1 million tissue biopsies in the USA performed under regional anaesthesia each year to diagnose cancer [2] and a survey showing approximately 50% of anaesthetists in the USA perform more than 100 spinal and epidural nerve blocks each year [3]. In these procedures, a needle is inserted deep into soft tissue to reach the target, with the accuracy of the insertion a key determinant of the success of diagnosis or effectiveness of treatment [4]. Ultrasound imaging is increasingly used for guidance in such procedures, to visualise anatomical structures of interest as well as the advancing needle. However, there is often a problem identifying the needle because the smooth surface of the shaft reflects incident ultrasound waves away from the imaging probe and the waves scattered back to the probe are too small to be detected. This problem is further exacerbated when needles are inserted at steep angles [5]. Percutaneous procedures with inadequate needle visualisation may result in failed or inaccurate diagnosis and serious complications such as vascular, neural or visceral injury [6,7]. In ultrasound-guided peripheral nerve block, repeated failure to visualise the needle tip was reported even by experienced clinicians who had performed more than 100 such procedures [8]. According to Liberman [9], 9–18% of biopsies performed by experienced operators are inadequate because of poor visualisation.

The risks associated with poor needle visibility have motivated a lot of research. Proposed improvements include advanced

* Corresponding author. Tel.: +44 (0)13823 85477.
E-mail address: z.y.huang@dundee.ac.uk (Z. Huang).

http://dx.doi.org/10.1016/j.ultras.2016.02.018
0041-624X/

imaging technologies such as beam steering [10] and 3D ultrasound imaging [11] to improve imaging quality; echogenic needles to increase the ultrasound waves scattered back to the imaging probe [12]; mechanical [13] and optical guidance [14] to optimise needle-beam-alignment; and observation of a vibrating needle under colour Doppler imaging [15]. All these technologies have specific abilities to improve needle visibility but they also all suffer from significant limitations and require further development. The use of colour Doppler imaging combined with a moving needle tip was accepted as one of the most promising methods to improve needle visibility [8]. The needle tip movement can be generated by manual motion of the needle [16], rotating a bent stylet within a needle [17], or piezoelectric actuators [15,18]. Gardineer and Vikomerson [19] patented a device termed a 'VIBRA', which uses a piezoelectric diaphragm to excite flexural vibrations of a needle and was later named ColorMark (EchoCath Inc., Princeton, NJ, USA). The ColorMark has been extensively used for laboratory and clinical trials, and significantly improved the needle visibility [15,20,21]. However, it was also found that the Doppler image tended to bleed into the tissue beyond the needle, resulting in difficulty in determining needle position accurately. The most probable reason for this is the nature of flexural vibration: the displacement is perpendicular to the propagation axis and thus the Doppler imaging of the needle expands beyond it. A similar device, which was based on the flexural vibration of a needle actuated by a piezoelectric buzzer, was reported elsewhere [18] and integrated into a 3-D tracking system [22].

Previously, one of the present authors proposed a ultrasound-actuated needle (USAN) to enhance needle visibility in cancer biopsy and regional anaesthesia procedures [23]. Unlike the aforementioned devices based on flexural vibration [18,19], the USNA uses the longitudinal vibration of a needle actuated by a piezoelectric transducer. Since the vibration in a longitudinal mode is confined within the needle, the Doppler response of the needle is substantially confined to the needle as well. However, flexural vibration of the needle was also excited and was found to induce strong artefacts in the needle images indicating that knowledge of the modal behaviour of the needle is required to tune the longitudinal mode, the topic on which this paper is focused. The present study was carried out with finite element modelling (FEM) and validated with experimental characterisation. It is demonstrated that a needle actuated with a tuned longitudinal mode produces clearer images with fewer artefacts than one operating in a flexural mode. Furthermore improved needle visibility was maintained while the needle was continuously advancing in a test specimen, indicating that real time tracking of the needle position is possible.

2. Ultrasound-actuated needle

The ultrasound-actuated needle (USAN) (Fig. 1) comprises a piezoelectric transducer coupled mechanically with a conventional surgical needle. In the piezoelectric transducer, two oppositely-polarised piezoelectric rings (PZ26, Meggitt Sensing Systems, Kvistgaard, Denmark) with electrodes on the flat surfaces, with outer diameter OD = 10 mm, inner diameter ID = 5 mm and thickness t = 2 mm, are sandwiched between a front mass and a back mass with a pre-stressed bolt. The main selection criteria for the piezoelectric rings were commercial availability and appropriate dimensions to give a compact size. The dimensions of the front mass were minimised, while the length of the back mass (22 mm) was chosen so that the displacement node of the transducer was positioned at the flange of the back mass. The purpose of the pre-stress is twofold: it applies a compressive stress to the piezoelectric material to avoid tensile stress in application since piezoelectric materials has low tensile strength (around 44–49 MPa [24]) and it ensures effective physical coupling between adjacent parts of the transducer. Two brass shims (not shown) serve as electrodes to supply electric signals to the transducer. The centre of the bolt was drilled out to a diameter D = 1.5 mm so that the needle can pass through the transducer. The front mass was designed with a collet which forms a collar around the needle and exerts a strong clamping force when it is tightened. It can accept needles in the range 0.8 mm < OD < 1.2 mm. The USAN is attached to a housing (not shown) through the flange on the back mass. When excited, the piezoelectric transducer actuates the needle to oscillate in a longitudinal vibration mode. As the minimum target depth reported for needle intervention procedures is 10–20 mm [15,25], and the transducer length is 55 mm including the housing (transducer itself 40 mm), this solution is applicable to needles greater than 65 mm in length. It will be possible to reduce the transducer length in future designs, thus reducing this constraint.

3. Finite element modelling

3.1. Modelling approaches

FEM was performed using Abaqus (Dassault Systems, Velizy-Villacoublay, France) based on frequency analysis, a standard procedure which extracts eigenvalues to calculate the natural frequencies and corresponding mode shapes of a system. When modelling the transducer, the brass shims used to supply the electrical signals were not included as their thickness (0.1 mm) was much less than the piezoelectric rings (2 mm). It was checked that this did not have a significantly deleterious effect on the accuracy of the results. As stated in Section 2, the main purposes of the pre-stress are to reduce the tensile stress to prevent the failure of the piezoelectric material and to ensure intimate mechanical contact between the components. As the failure mechanism of the piezoelectric material was not included in the FEM and all the components of the transducer were bonded together ideally, the pre-stress was not considered. Opposing poling directions were specified for the two piezoelectric rings, as required in this multilayer design, and all electrodes were specified with zero potential. The input material properties are listed in Table 1.

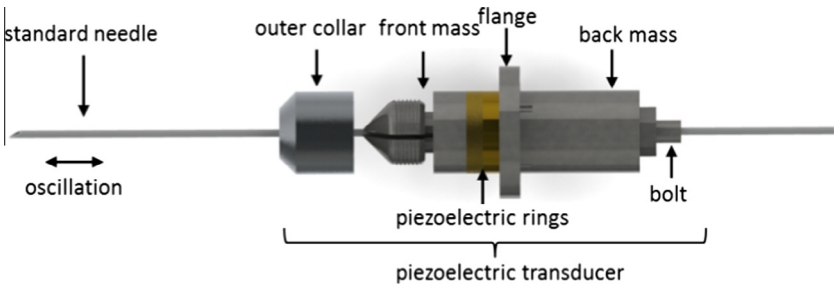

Fig. 1. A schematic of the ultrasound-actuated needle configuration.

Table 1
Input material parameters used in FEM.

Front mass: aluminum	
Young's modulus (GPa)	71.7
Poisson's ratio	0.33
Density (kg/m^3)	2800
Back mass/needle: stainless steel	
Young's modulus (GPa)	210
Poisson's ratio	0.3
Density (kg/m^3)	7850
Piezoelectric material: PZ 26	
Stiffness constants (GPa)	
C_{11}^E	168
C_{12}^E	110
C_{13}^E	99.9
C_{33}^E	123
C_{44}^E	30.1
Piezoelectric constants (C/m^2)	
e_{31}	−2.8
e_{33}	14.7
e_{24}	9.86
Relative dielectric constants	
ε_{11}^T	1190
ε_{33}^T	1330
Density (kg/m^3)	7700

Fig. 2. 3D model of a 21-gauge standard anaesthetic needle with 30° facet bevel.

The specific application of a needle used for regional anaesthesia and tissue biopsy dictates its length, diameter, tip geometry and material; here, 21 gauge needles commonly used for regional anaesthesia were selected, with OD = 0.9 mm and a 30° facet bevel at the tip (Fig. 2). The material was stainless steel with the properties shown in Table 1. Considering the overall tubular geometry, in the work described here it was assumed that only the needle length significantly affected its modal behaviour, and the needle hub and the cartridge end were ignored. The vibration modes of the needle were simulated under free boundary conditions.

The complete USAN device comprises the needle and the piezoelectric transducer coupled together. The contact areas between the needle and the collet of the front mass were bonded together. Again zero potential was specified on all the transducer electrodes.

3.2. FEM results and discussion

3.2.1. Transducer and needle modes

The longitudinal mode shape of the transducer alone is shown in Fig. 3, neglecting the outer collar, at the longitudinal resonance frequency, f_{rlt} = 52 kHz. The maximum vibration amplitude is located at the tip of the front mass and the nodal plane is at the flange.

A freely vibrating needle supports three types of vibration mode: torsional, flexural and longitudinal, as shown in Fig. 4. Torsional modes are characterised by angular vibration along the needle length and are difficult to excite using a longitudinal mode transducer [26]; thus, they are not discussed here. In a longitudinal mode, the dominant motion is along the needle length whereas, in a flexural mode, the dominant motion is perpendicular to the needle length. It has also been noted that for a flexural mode, maximum flexural displacement is usually located at the needle tip, probably caused by the asymmetric geometry. In practice, it is quite common for longitudinal and flexural motion to be coupled together in one mode. Here, a mode is regarded as longitudinal

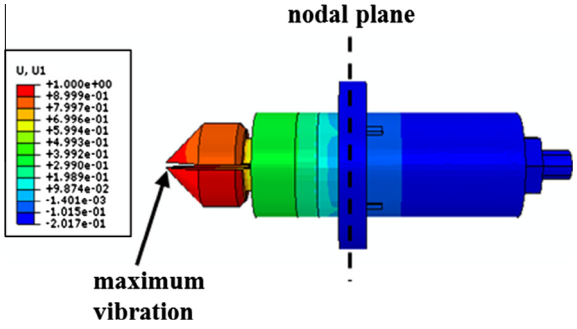

Fig. 3. Longitudinal mode shape of the piezoelectric transducer at 52 kHz: u1 is the normalised longitudinal displacement.

when its maximum longitudinal displacement is three times larger than the maximum flexural displacement.

Fig. 5 shows the first and second longitudinal resonance frequencies of needles with the design featured in Section 3.1 but with different lengths. The first resonance frequency decreases from 64 kHz to 20 kHz when the length increases from 40 mm to 120 mm and the second longitudinal resonance frequency decreases almost exactly proportionately the same from 130 kHz to 41 kHz.

When the transducer is coupled with a needle, three different longitudinal vibration modes are possible, as illustrated in Fig. 6, representing a needle 100 mm long gripped by the transducer at a distance 45 mm from the tip. This grip position allows maximum needle penetration into tissue, taking into account the 55 mm total length of the transducer and housing. The lowest frequency mode, at f_{rln} = 21.7 kHz has its maximum displacement at the end of the needle, and is thus termed a proximal mode here. There is also a mode, f_{rln} = 26.7 kHz, with its maximum displacement at the tip of the needle, hence termed a distal mode. Both distal and proximal modes show the minimum displacement at approximately 45 mm from the needle tip because the needle is clamped by the transducer at this position. Finally, there is a mode, f_{rln} = 52.1 kHz, with its maximum displacement half-way along the needle. This corresponds closely to the second longitudinal mode of the freely vibrating needle and is here termed a transducer mode. Since high vibrational amplitude at the tip is desirable for needle actuation, giving greater engagement with the tissue under penetration, the distal and transducer modes are more suitable for the present application than the proximal mode and are discussed further below.

3.2.2. Effect of needle length and grip position

To study the effect of the needle length and grip position on the resonance frequency and mode shape, needles of lengths 100 mm and 120 mm were attached to the piezoelectric transducer. With each needle, the grip position, defined as the distance from the needle tip to the position where the needle is gripped by the transducer, was varied from 40 to 80 mm. The resonance frequencies and corresponding mode shapes were computed at each grip position using FEM frequency analysis, with the longitudinal modes summarised in Table 2. The distal mode existed with both needle lengths at all grip positions, with the resonance frequency decreasing as the grip position increased. At corresponding grip positions, the frequencies were similarly for both the 100 mm and 120 mm needles. This suggests that the distal mode always exists regardless of needle length and grip position and that its frequency is independent of the total needle length and varies only with the grip position.

The transducer mode was observed only with the 100 mm needle and always at 52.1 kHz. With the 120 mm needle, the USAN as a whole still resonated at 52.1 kHz, but as a combination of a

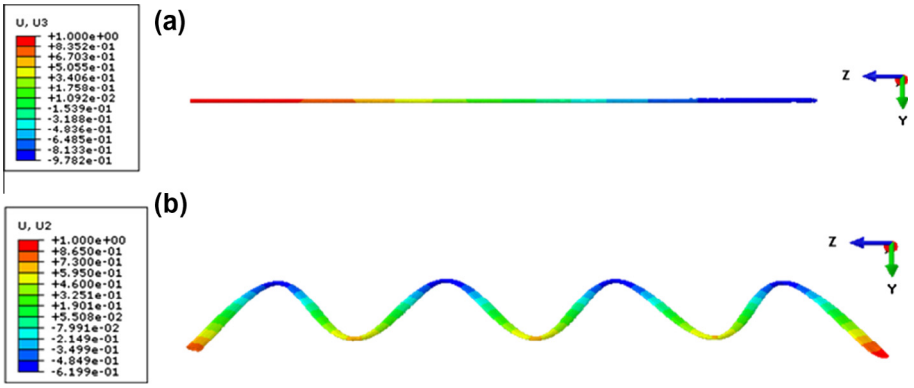

Fig. 4. Vibration modes of a freely vibrating needle with a length of 100 mm, (a) longitudinal mode at 25.2 kHz and (b) flexural mode at 10.4 kHz.

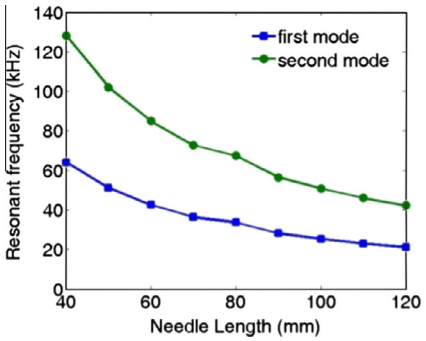

Fig. 5. The first and second longitudinal resonance frequencies of freely vibrating needles of different lengths.

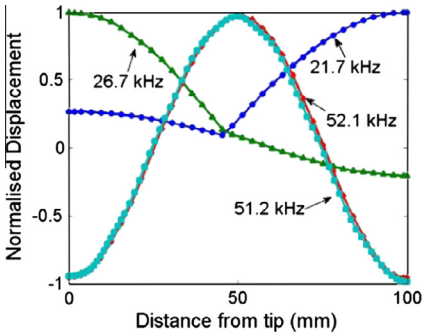

Fig. 6. Normalised displacement along the needle length: frequencies of 21.7 kHz, 26.7 kHz and 52.1 kHz correspond to longitudinal "proximal", "distal" and "transducer" modes, respectively, with a 100 mm needle gripped 45 mm from tip; the frequency of 51.2 kHz corresponds to the second longitudinal mode of the freely vibrating needle.

Table 2
The longitudinal mode resonance frequencies of the transducer coupled to needles of two different lengths gripped at several different positions, simulated with FEM.

Grip position (mm)	Distal modes	
	100 mm needle (kHz)	120 mm needle (kHz)
40	29.6	30.0
45	26.7	28.2
50	22.8	23.5
60	20.0	20.9
70	17.3	18.0
80	15.3	15.3

longitudinal transducer mode and a flexural needle mode as illustrated in Fig. 7. This is because, when the transducer is excited at resonance, it actuates the needle to vibrate at the same frequency. If this frequency matches f_{rln}, as in the case of the 100 mm needle, f_{rln} = 53 kHz, the vibration mode of the needle is longitudinal. Otherwise, the vibration mode of the needle is flexural, as in the case of the 120 mm needle (f_{rln} = 40 kHz).

3.2.3. Longitudinal vibration modes of the USAN

Taking into account the results from the previous section, a 100 mm long needle was chosen as most suitable for further analysis, gripped 45 mm from the tip. Frequency analysis revealed three distinct longitudinal vibration modes which are explained below. The longitudinal displacement of the three modes along the needle length has been shown in Fig. 6 and the lowest order mode of each type is presented in Fig. 8. At both f_{rln} = 21.7 kHz and f_{rln} = 26.7 kHz, the needle was longitudinally resonant but the transducer was not resonant. At 21.7 kHz, the proximal end showed much higher displacement (normalised as 1) than the distal tip (normalised as −0.25) and the converse was true at 26.7 kHz. Higher order harmonics exist for both these modes but only the lowest order modes are discussed here. At f_{rln} = f_{rlt} = 52.1 - kHz, both the needle and the transducer were resonant. In this mode, the needle tip and end exhibited the same motion amplitude. Further, the longitudinal displacement profile of the 100 mm needle actuated by the transducer was the same as the 100 mm needle in free vibration, as shown in Fig. 6.

4. Experimental characterisation

4.1. Experimental setup

The bespoke testing arrangement shown in Fig. 9 was used to measure the electric impedance characteristics and vibration response of the transducer and the USAN. The system is able to perform frequency sweeping at different voltage levels up to 20 V_{pp}, limited by the signal generator, and this can be increased by using a power amplifier. This is not a standard function provided by instruments such as an impedance analyser. A description of the system's development as well as its calibration is given elsewhere [27]. It comprises a data acquisition system (NI PXIe 5122 and 6124 on NI PXIe 1082 chassis, National Instruments, Newbury, Berks, UK), a signal generator (33220A, Agilent Technologies, Santa Clara, USA), a current probe (P602, Tektronix, Bracknell, UK) and a voltage probe (N2862B, Agilent Technologies, Santa Clara, USA). A PC controls the signal generator to output sinusoidal frequency sweep signals to the USAN. The voltage across and the current through the USAN are sampled by the voltage probe and the current probe respectively. The sampled signals are digitised by the NI PXIe 5122 and used to calculate the electric impedance. Simultaneously, the vibration amplitude of the needle, either longitudinal or flexural, is measured by a laser Doppler vibrometer (OFV2570 and OFV 534, Polytec, Herts, UK) then digitised by the NI PXIe 6124.

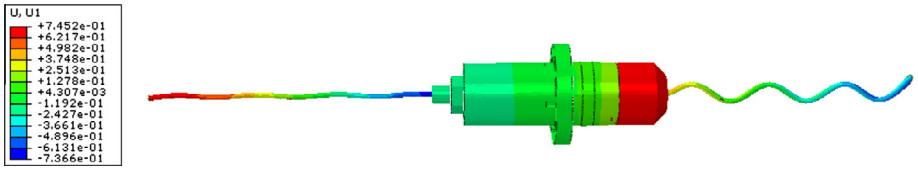

Fig. 7. Mode shape of the needle actuating device at 52.1 kHz when a 120 mm needle was gripped at 45 mm from tip: u1 is the longitudinal displacement.

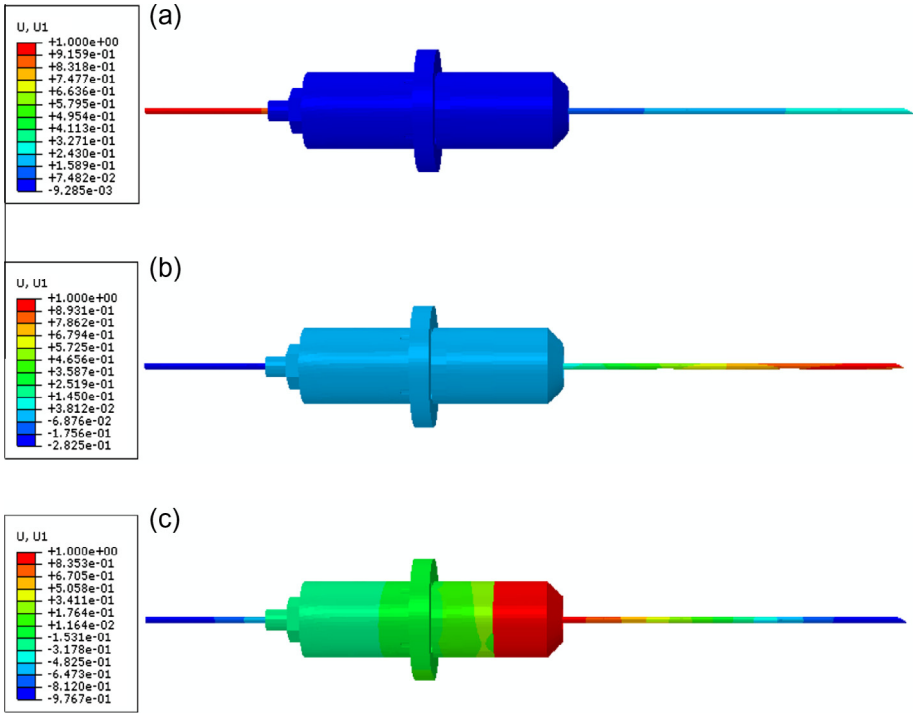

Fig. 8. The first three longitudinal vibration modes with a 100 mm long needle gripped 45 mm from the needle tip: (a) proximal mode at 21.7 kHz, (b) distal mode at 26.7 kHz and (c) transducer mode at 52.1 kHz.

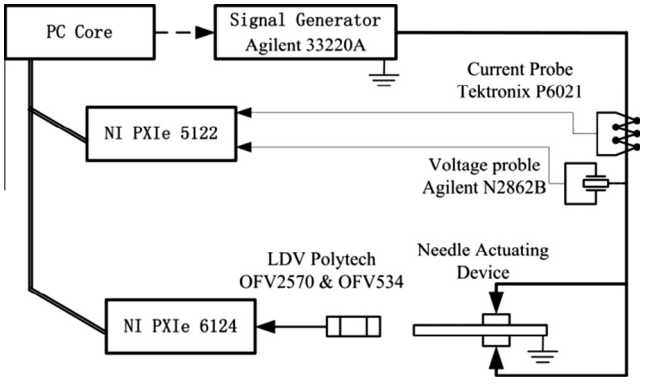

Fig. 9. Schematic of the experimental characterisation setup.

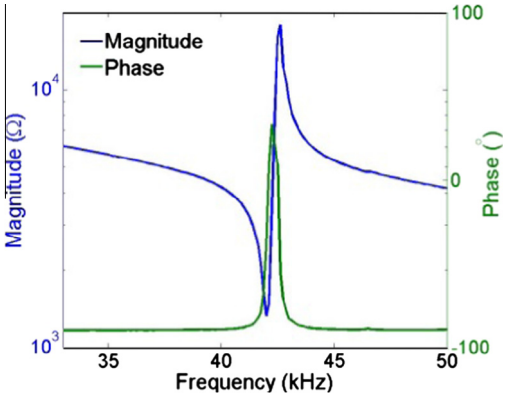

Fig. 10. The electric impedance spectrum of the transducer.

4.2. Results and discussion

4.2.1. Vibration mode of the transducer

Experimentally, the resonance frequency of the piezoelectric transducer was f_{rlt} = 42 kHz, as indicated by the electric impedance spectrum in Fig. 10. The discrepancy of 10 kHz compared with the simulation result is attributed to three effects: (1) manufacturing imperfections; (2) differences between the actual parameters of the piezoelectric materials and the data provided by the supplier (±5% as indicated by the supplier); and most importantly (3) the limited effective coupling area between adjacent components of the transducer, because only a limited torque and thus a limited pre-stress was applied to the bolt. It has been stated that the effective coupling area between the transducer components initially increases with pre-stress then gradually stabilises at the maximum value when the pre-stress is higher than 30–45 MPa [28]; as a result and accordingly, the resonance frequency of the transducer initially increases with the pre-stress and then stabilises. In simulation, the contact areas between adjacent components in the transducer were bonded together ideally, resulting in the maximum possible coupling area. In practice, the torque applied

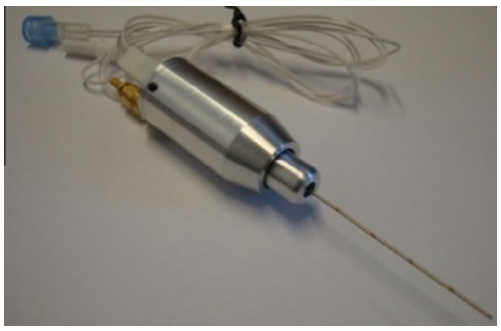

Fig. 11. USAN with a 120 mm regional anaesthesia needle.

to tighten the transducer components together was limited to reduce the risk of breaking the hollow bolt through which the needle is inserted. The limited torque resulted in a limited pre-stress (<20 MPa) and consequently a reduced effective coupling area. Therefore, the resonance frequency in practice is lower than simulation.

4.2.2. Longitudinal vibration modes of the USAN

A 120 mm long needle of the type used here has a longitudinal resonant mode at 40 kHz, as shown in Fig. 5; therefore, contrary to simulation, a 120 mm anaesthetic needle was inserted into the transducer, as shown in Fig. 11. Fig. 12(a) shows the longitudinal displacement measured by the LDV, at both distal and proximal ends of the needle, when the grip position was 45 mm (keeping the same grip position as simulation) and the transducer was excited at 5 V_{pp}, and Fig. 12(b) shows the electrical impedance spectrum.

Three resonant modes were found at frequencies below 45 kHz, located at 16.5 kHz, 27.6 kHz and 42.2 kHz respectively. In simulation, it is straightforward to identify the longitudinal and flexural modes, since the displacements in all directions can be interrogated. However, in experimental characterisation, it is necessary to measure the flexural displacement of the needle separately and compare it with the longitudinal displacement to identify the mode type. This was done by measuring the displacement normal to the needle axis with the LDV, point by point along the needle length with 1 mm resolution, for the 27.6 kHz and 42.2 kHz modes, since both modes showed relatively high longitudinal displacement at the needle tip (0.96 μm for the 27.6 kHz mode and 0.45 μm for the 42.2 kHz mode), which is desirable for the present application. The flexural displacement of the 16.5 kHz mode was not measured because this mode generated no longitudinal vibration at the needle tip. Measurements were taken from the needle tip to the grip position since the needle tip generates the maximum flexural displacement, as observed in simulation. It should also be noted from Fig. 12(b) that the 42.2 kHz mode has much lower electric impedance (1.06 kΩ) than both the 16.5 kHz (11.4 kΩ) and the 27.6 kHz (6.2 kΩ) modes, with the 16.5 kHz mode so weak that it cannot be seen in the impedance spectrum. Fig. 13 presents the flexural displacement along the needle length for the 27.6 kHz and 42.2 kHz modes.

Finite amplitudes of flexural displacement were observed at both frequencies. However, the amplitude of the longitudinal displacement at the tip was 10 times larger than the maximum flexural displacement, indicating that both modes were longitudinal. Moreover, the 27.6 kHz mode was identified as a distal mode, since the distal tip showed much higher displacement than the proximal end of the LDV scan, as indicated in Fig. 12(a). This agrees well with the resonance frequency predicted by the simulation, which is 26.7 kHz. The 42.2 kHz mode was identified as a transducer mode because, most obviously, the transducer was resonant at 42.2 kHz as indicated by the impedance spectrum in Fig. 12(b) but also

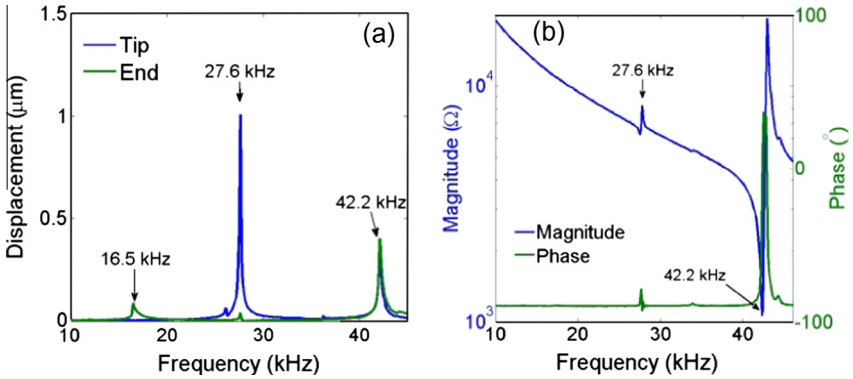

Fig. 12. Characteristics of USAN with a 120 mm needle gripped at 45 mm from needle tip. (a) longitudinal displacement at the needle tip and the needle end and (b) electric impedance.

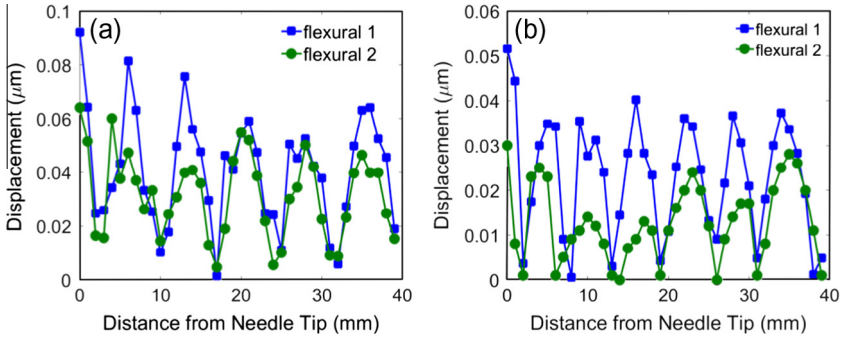

Fig. 13. Amplitude of flexural displacements along the needle length when USAN was excited at 5 V. (a) f = 27.6 kHz and (b) f = 42.2 kHz; "flexural 1" and "flexural 2" are normal to the needle length and mutually orthogonal.

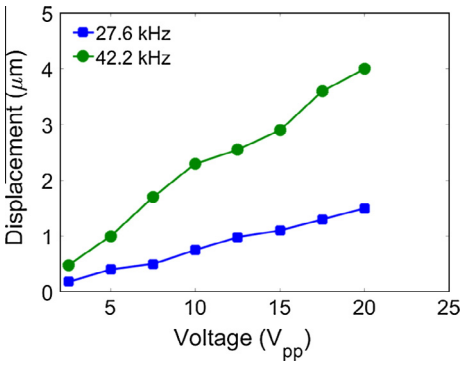

Fig. 14. The longitudinal vibration of the needle tip measured at different voltage.

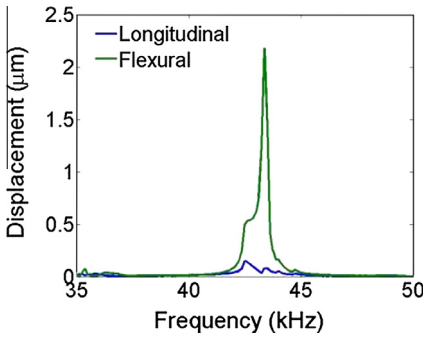

Fig. 15. Longitudinal and flexural displacement components at the tip of a 100 mm needle gripped by the transducer at 45 mm.

because the needle tip and end both exhibit the same longitudinal vibration amplitude as indicated in Fig. 12(a). The 16.5 kHz mode was identified as a proximal mode because the longitudinal displacement of 0.1 μm was detected at the proximal end but not at the needle tip, where it was too small to detect by the LDV, in agreement with the characteristics of a proximal mode as discussed in Section 3.2.3. Fig. 14 presents the longitudinal vibration of the needle tip measured at different actuating voltages. The vibration amplitudes at both 27.6 and 42.2 kHz increase linearly with voltage. At 20 V_{pp}, the 26.7 kHz mode has a vibration amplitude of 4 μm, whereas the 42.2 kHz mode has a vibration amplitude of 1.5 μm.

4.2.3. Effects of needle length and grip position

To investigate the effects of grip position and needle length on the longitudinal vibration modes experimentally, two anaesthetic needles of lengths 100 and 120 mm respectively were gripped by the transducer at different positions. At each grip position, the longitudinal displacement at the needle tip was measured. Then the resonance frequencies were identified from the displacement–frequency curve and flexural displacement along the needle at those frequencies was measured and compared with longitudinal displacement to identify the mode type.

The longitudinal resonance frequencies are summarised in Table 3 and compared with the simulation results. For the distal mode, the experimental results agree well with the simulation and confirm that this mode is always available, regardless of the total needle length and grip position. This eliminates the need to select needles of a specific total length to match the transducer. Even though the longitudinal mode shape is independent of the grip position, the position must still be carefully set since it affects the resonance frequency. A negative aspect of the distal mode is that the electric impedance magnitude is very high (6.2 kΩ), making practical impedance matching with the power source (50 Ω impedance) difficult.

Experimentally, the transducer mode was available only with the 120 mm needle. When working with the 100 mm needle, the

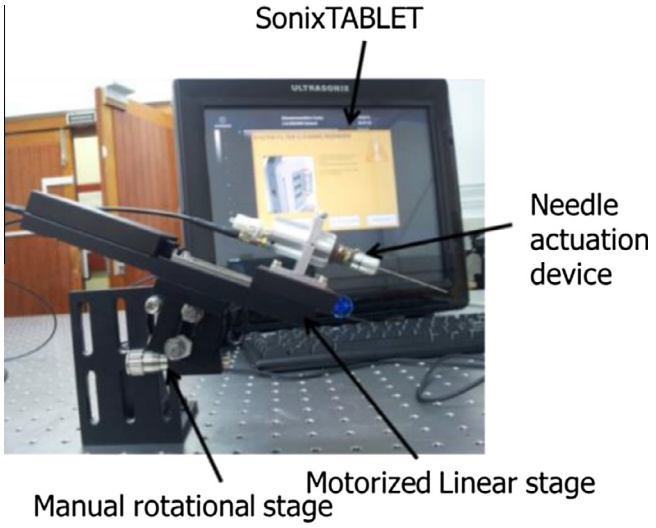

Fig. 16. The experimental setup for the needle visibility tests.

vibration modes around 42 kHz were flexural. A representative response of the needle tip motion under the influence of these flexural modes is shown in Fig. 15, depicting the longitudinal and flexural displacements at the needle tip against frequency. At 42 kHz, the flexural displacement was 0.49 μm compared with a longitudinal displacement of approximately 0.1 μm confirming the mode is flexural. The transducer mode frequency fluctuated around 42 kHz, with the small variations attributed to differing torques applied when tightening the outer collar of the transducer.

The transducer mode is available only when the resonance frequency of the transducer matches the longitudinal resonance frequency of a freely vibrating needle. Because the longitudinal resonance frequency of the needle is determined mainly by its total length, only needles of specific lengths can be used for one particular transducer to obtain the transducer mode. However, the resonance frequency and mode shape are independent of the

Table 3
The longitudinal resonance frequencies of the USAN including needles of different lengths gripped at different positions: EXP. are experimental results; SIM. are simulation results.

Grip position (mm)	Distal mode				Transducer mode			
	100 mm needle (kHz)		120 mm needle (kHz)		100 mm needle (kHz)		120 mm needle (kHz)	
	EXP.	SIM.	EXP.	SIM.	EXP.	SIM.	EXP.	SIM.
40	28.8	29.6	29.4	30.0	N/A	52.1	42.5	N/A
45	27.6	26.7	27.8	28.2	N/A	52.1	42.2	N/A
50	23.3	22.8	23.5	22.5	N/A	52.1	41.4	N/A
60	19.7	19.9	19.7	20.9	N/A	52.1	41.8	N/A
70	16.8	17.3	16.8	18.0	N/A	52.1	42.0	N/A
80	14.9	15.2	14.9	15.3	N/A	52.1	41.7	N/A

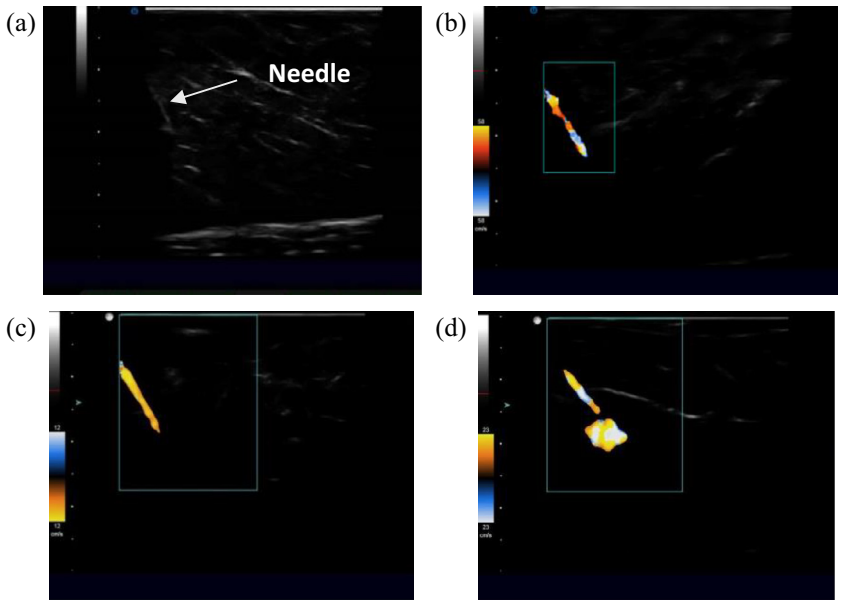

Fig. 17. Ultrasound images of the USAN (a) grey scale ultrasound image without ultrasonic actuation on the needle; colour Doppler images of the actuated needle in (b) transducer mode, (c) needle distal mode and (d) flexural mode. (For interpretation of the references to colour in this figure legend, the reader is referred to the web version of this article.)

grip position, which is convenient in practice because the grip position does not require careful setting. Whilst the electrical impedance of the transducer mode (1.06 kΩ) is less than for the distal mode (6.2 kΩ), both are still far from the 50 Ω impedance of the power source.

5. Needle visibility tests

5.1. Setup

Following basic experimental characterisation of the USAN, further experiments were carried out to test needle visibility under colour Doppler imaging using the arrangement in Fig. 16. The USAN was mounted on a motorised linear translation stage (MTS50-Z8, THORLABS Ltd., Ely, Cambs, UK) to ensure repeatable results. The linear translation stage, mounted on a rotational stage, can provide a maximum displacement of 50 mm at a peak velocity of 3 mm/s. With the two stages, the insertion angle and insertion depth of the needle can be controlled precisely and repeatably. An ultrasound imaging system (SonixTablet, Ultrasonics, Richmond, Canada) with a 5 MHz flat linear ultrasound imaging probe was used to visualise the needle in fresh porcine specimens. The study was carried out using the in-plane approach in which the needle is inserted in the plane of the ultrasound beam and should be visible as a bright hyperechoic line [29]. The insertion depth was 30 mm, and the insertion angle 60°.

The USAN was excited by a bespoke driving system with resonance tracking capability [27] in distal, transducer and flexural modes. The distal mode (f_{rln} = 27.6 kHz) and the transducer mode (f_{rlt} = 42.2 kHz) were generated by the USAN with a 120 mm anaesthetic needle gripped at 45 mm from the tip. The flexural mode (f_{rfn} = 42.0 kHz) was generated by the USAN with a 100 mm anaesthetic needle, also gripped at 45 mm. The actuating voltage was increased from 2 V_{pp} until the whole needle was visible.

5.2. Results and discussion

Initially, conventional grey scale ultrasound imaging of the USAN without actuation was captured as shown in Fig. 17(a) matching present practice in ultrasound-guided percutaneous procedures. Whilst the shaft of the needle can be seen, it is not very clear and the position of the needle tip can be identified only with difficulty.

Colour Doppler images of the USAN working at the longitudinal vibration modes are shown in Fig. 17(b) and (c), where the distal and transducer modes were excited at 12 V_{pp} and 14 V_{pp} respectively. In both figures, the needle is visible as a continuous, coloured line including both the shaft and the tip. The minimum voltage found to highlight the whole needle was 12 V_{pp} for the transducer mode and 14 V_{pp} for the distal mode, corresponding to vibration amplitudes of 0.95 μm and 3 μm measured in air, respectively. The higher voltage and vibration required for the distal mode may be because its vibration was attenuated more significantly by the tissue. However, this attenuation could not be evaluated experimentally because the vibration occurs in tissue, which is inaccessible to LDV. In Fig. 17(d), using the flexural mode, the needle shaft was still highlighted but very strong artefacts were generated around the needle tip making its position impossible to localise accurately. This is because vibration in a flexural mode is perpendicular to the needle axis and thus not confined within the needle, in turn eliciting a potentially misleading Doppler response beyond the needle.

Images of the actuated needle recorded in real time.

Images during needle insertion and withdrawal were recorded in real time on the imaging system when the 120 mm needle was actuated in the transducer mode, as shown in Video.

The needle advances to a depth of 30 mm in the first 20 s and is clearly visualised in colour Doppler mode, allowing the tip position to be tracked. The sudden disappearance of the needle image at 9 s is explained by misalignment between the ultrasound probe and the needle. At 30 s, the imaging system is switched to grey-scale mode (B-mode) and the needle image disappears. As soon as colour Doppler mode is restored at 35 s, the needle becomes visible again. The needle is then withdrawn slowly from the specimen, still with successful visualisation, and its position can be monitored in real time.

6. Conclusions

This paper has reported the effects of modal behaviour of an ultrasound-actuated needle developed to improve needle visibility by exciting vibration in the needle and imaging this using colour Doppler. The study was performed using FEM and validated by experimental characterisation. When actuated by a longitudinal-mode transducer, the needles exhibited three specific longitudinal vibration mode types that have been termed the transducer mode, the distal mode and the proximal mode. Both the distal mode and the transducer mode generated high amplitudes of motion at the needle tip and were therefore selected as most suitable for the application. The transducer mode was available only when the longitudinal resonance frequency of the needle matched the transducer. Its frequency was determined by the transducer, independent of the position at which the needle was gripped. As the longitudinal resonance frequency of a needle is dependent on its total length, a transducer can only work with needles in specific lengths in this mode. The distal mode can be excited in any needle, with its frequency decreasing as the grip position is moved away from the needle tip. The USAN, combined with colour Doppler imaging, significantly improved needle visibility, with the longitudinal vibration of the needle producing clear images with few artefacts, allowing the position of the needle to be monitored continuously in real time. Further practical work will reduce the transducer dimensions and improve the housing design to improve it ergonomically and clinical investigations will then be performed.

Acknowledgements

Mr Yang Kuang was supported by the China Scholarship Council and University of Dundee.

References

[1] H. Kehlet, J.B. Dahl, Anaesthesia, surgery, and challenges in postoperative recovery, The Lancet 362 (2003) 1921–1928.
[2] L.E. Hoorntje, P.H.M. Peeters, W. Mali, I. Rinkes, Vacuum-assisted breast biopsy: a critical review, Eur. J. Cancer 39 (August) (2003) 1676–1683.
[3] R. Brull, D.S. Wijayatilake, A. Perlas, V.W. Chan, S. Abbas, G.A. Liguori, et al., Practice patterns related to block selection, nerve localization and risk disclosure: a survey of the American Society of Regional Anesthesia and Pain Medicine, Reg. Anesth. Pain Med. 33 (2008) 395–403.
[4] J.H. Youk, E.-K. Kim, M.J. Kim, K.K. Oh, Sonographically guided 14-gauge core needle biopsy of breast masses: a review of 2,420 cases with long-term follow-up, Am. J. Roentgenol. 190 (2008) 202–207. 2008/01/01.
[5] T. Maecken, M. Zenz, T. Grau, Ultrasound characteristics of needles for regional anesthesia, Reg. Anesth. Pain Med. 32 (2007) 440–447.
[6] D. Dillane, B. Finucane, Local anesthetic systemic toxicity, Can. J. Anesth./J. canadien d'anesthésie 57 (2010) 368–380. 2010/04/01.
[7] R. Brull, C.J. McCartney, V.W. Chan, H. El-Beheiry, Neurological complications after regional anesthesia: contemporary estimates of risk, Anesth. Analg. 104 (2007) 965–974.
[8] K.J. Chin, A. Perlas, V.W.S. Chan, R. Brull, Needle visualization in ultrasound-guided regional anesthesia: challenges and Solutions, Reg. Anesth. Pain Med. 33 (2008) 532–544.
[9] L. Liberman, Percutaneous imaging-guided core breast biopsy: state of the art at the millennium, Am. J. Roentgenol. 174 (2000) 1191–1199.
[10] J.A. Baker, M.S. Soo, P. Mengoni, Sonographically guided percutaneous interventions of the breast using a steerable ultrasound beam, AJR Am. J. Roentgenol. 172 (1999) 157–159.
[11] S. Cheung, R. Rohling, Enhancement of needle visibility in ultrasound-guided percutaneous procedures, Ultrasound Med. Biol. 30 (2004) 617–624.
[12] S. Hebard, G. Hocking, Echogenic technology can improve needle visibility during ultrasound-guided regional anesthesia, Reg. Anesth. Pain Med. 36 (2011) 185–189, http://dx.doi.org/10.1097/AAP.0b013e31820d4349.
[13] J. Kettenbach, G. Kronreif, M. Figl, W. Birkfellner, R. Hanel, H. Bergmann, Robot-assisted biopsy using ultrasound guidance: initial results from in vitro tests, Eur. Radiol. 15 (2005) 765–771.
[14] B.C.H. Tsui, Facilitating needle alignment in-plane to an ultrasound beam using a portable laser unit, Reg. Anesth. Pain Med. 32 (2007) 84–88.
[15] R. Feld, L. Needleman, B.B. Goldberg, Use of needle-vibrating device and color Doppler imaging for sonographically guided invasive procedures, AJR Am. J. Roentgenol. 168 (1997) 255–256.
[16] U.M. Hamper, B.L. Savader, S. Sheth, Improved needle-tip visualization by color Doppler sonography, AJR Am. J. Roentgenol. 156 (1991) 401–402.
[17] A. Harmat, R.N. Rohling, S.E. Salcudean, Needle tip localization using stylet vibration, Ultrasound Med. Biol. 32 (2006) 1339–1348.
[18] S.M. Klein, M.P. Fronheiser, J. Reach, K.C. Nielsen, S.W. Smith, Piezoelectric vibrating needle and catheter for enhancing ultrasound-guided peripheral nerve blocks, Anesth. Analg. 105 (2007) 1858–1860.
[19] B. Gardineer, D. Vilkomerson, Apparatus and method for locating an interventional medical device with a ultrasound color imaging system, Google Patents, 1994.
[20] G. Armstrong, L. Cardon, D. Vilkomerson, D. Lipson, J. Wong, L. Leonardo Rodriguez, et al., Localization of needle tip with color doppler during pericardiocentesis: In vitro validation and initial clinical application, J. Am. Soc. Echocardiogr. 14 (2001) 29–37.
[21] C.D. Jones, J.P. McGahan, K.J. Clark, Color Doppler ultrasonographic detection of a vibrating needle system, J. Ultrasound Med. 16 (1997) 269–274.
[22] M.P. Fronheiser, S.W. Smith, Analysis of a vibrating interventional device to improve 3-D colormark tracking, Ultrason. Ferroelectr. Freq. Control IEEE Trans. 54 (2007) 1700–1707.
[23] M. Sadiq, Enhanced biopsy and regional anaesthesia through ultrasound actuation of a standard needle, University of Dundee, 2013.
[24] T. Fett, D. Munz, G. Thun, Tensile and bending strength of piezoelectric ceramics, J. Mater. Sci. Lett. 18 (1999) 1899–1902.
[25] R.H. Gottlieb, W.B. Robinette, D.J. Rubens, D.F. Hartley, P.J. Fultz, M.R. Violante, Coating agent permits improved visualization of biopsy needles during sonography, Am. J. Roentgenol. 171 (1998) 1301–1302.
[26] M. Lucas, J.N. Petzing, A. Cardoni, L.J. Smith, J.A. McGeough, Design and characterisation of ultrasonic cutting tools, CIRP Ann. – Manuf. Technol. 50 (2001) 149–152.
[27] Y. Kuang, Y. Jin, S. Cochran, Z. Huang, Resonance tracking and vibration stablilization for high power ultrasonic transducers, Ultrasonics 54 (2014) 187–194.
[28] F.J. Arnold, S.S. Mühlen, The resonance frequencies on mechanically pre-stressed ultrasonic piezotransducers, Ultrasonics 39 (2001) 1–5.
[29] G. Corner, C. Grant, Peripheral nerve location techniques, Princ. Pract. Reg. Anaesth. (2012) 88.